

Electrical and photoconductive properties of vertical ZnO nanowires in high density arrays

Zhiyong Fan, Deepanshu Dutta, Chung-Jen Chien, Hsiang-Yu Chen, and Evan C. Brown
Department of Chemical Engineering and Materials Science, University of California-Irvine, Irvine, California 92697

Pai-Chun Chang and Jia G. Lu^{a)}
Department of Electrical Engineering, University of Southern California, Los Angeles, California 90089
and Department of Physics and Astronomy, University of Southern California, Los Angeles, California 90089

(Received 23 June 2006; accepted 3 October 2006; published online 22 November 2006)

High density vertical zinc oxide nanowire arrays were fabricated using highly ordered channels in anodic alumina membranes via chemical vapor deposition assisted by electrochemical deposition methods. Using conductive atomic force microscopy, the electrical transport and photoconduction of individual vertical nanowires were investigated. A negative photoconductivity was observed as a result of electron trapping in the alumina membrane. In contrast, positive photoconductivity was observed using a thermally annealed anodic alumina membrane as the nanowire growth template. These studies provide a pathway for constructing highly integrated nanoscale electronic and optoelectronic circuits, such as logic circuits, light emitting diodes, solar cells, and ultrahigh resolution imaging sensors. © 2006 American Institute of Physics. [DOI: 10.1063/1.2387868]

In recent years, quasi-one-dimensional (Q1D) semiconducting nanostructures have attracted tremendous interest for their unique physical properties attributed to their small dimensions. Driven by their enticing potential as nanoscale building blocks for integrated electronic and photonic circuits, much effort has been invested in the fabrication and characterization of functional devices based on Q1D nanostructures, such as field-effect transistors, sensors, lasers, solar cells, etc. In parallel, integration of device elements has been explored by both top-down and bottom-up techniques. In order to fully utilize the scaling advantage of the Q1D structures, vertical alignment provides an efficient and flexible way to construct three-dimensional (3D) architectures. In fact, 3D architecture using semiconducting nanowires as scaffolds has been utilized for building dye-sensitized solar cells,¹ vertical field-effect transistors,² and field-emission devices.³ In most of the previous reports, vertical Q1D semiconducting materials were grown on epitaxial substrates. The control of their horizontal ordering and density requires complex process.^{4,5} In addition, the resulting Q1D arrays are freestanding, thus posing difficulty to fabricate “bottom” and “top” electrodes to address individual Q1D channels. In this work, a high density ZnO nanowire array was assembled into an anodic alumina membrane (AAM) via the chemical vapor deposition (CVD) method assisted by electrodeposition of tin (Sn) catalysts. The electrical transport and photoconduction of individual vertical ZnO nanowires were characterized using conductive atomic force microscopy (AFM). This study provides a pathway for implementing integrated nanoscale electronics and optoelectronics using highly ordered nanowire arrays.

AAM has been widely used as a template for fabrication and direct assembly of a variety of Q1D nanostructures.^{6–8} Its advantage rests in the convenience of controlling the as-

pect ratio as well as the integration density. In this work, 2.5 μm thick AAMs were fabricated using a two-step anodization method. In brief, aluminum chips were first electropolished at 25 °C in a 1:3 mixture of perchloric acid and ethanol for 5 min then anodized in 0.3 M oxalic acid at 5 °C and 60 V for 3 h. The synthesized AAM layer was removed in a mixture of phosphoric acid (6 wt %) and chromic acid (1.5 wt %). The second anodization was then performed for 16 min under the same condition to achieve hexagonally ordered pores with interpore distance around 150 nm, as shown in the field-emission scanning electron microscope (FESEM) image in Fig. 1. In order to carry out the subsequent catalyst electrodeposition, a current ramping process⁹ was carried out to decrease the AAM barrier thickness. Such process usually creates dense subchannels in the barrier layer as displayed in the inset of Fig. 1.

ZnO nanowires were synthesized into the AAM nanochannels using electrodeposition followed by laser ablation assisted CVD process. The nanowire growth and contact

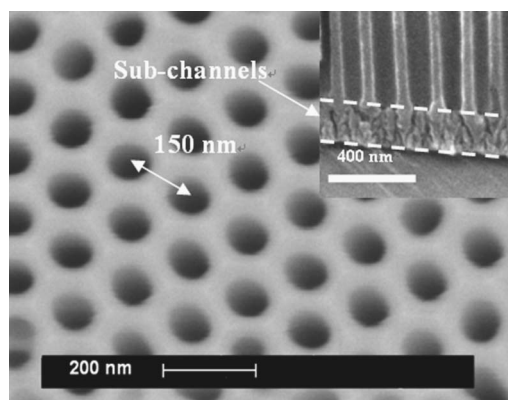


FIG. 1. FESEM image of an AAM anodized at 60 V to obtain 150 nm interpore distance. Inset: cross section of the AAM showing vertical channels and subchannels formed in the barrier layer (region bounded by the dashed lines).

^{a)} Author to whom correspondence should be addressed; electronic mail: jjalu@usc.edu

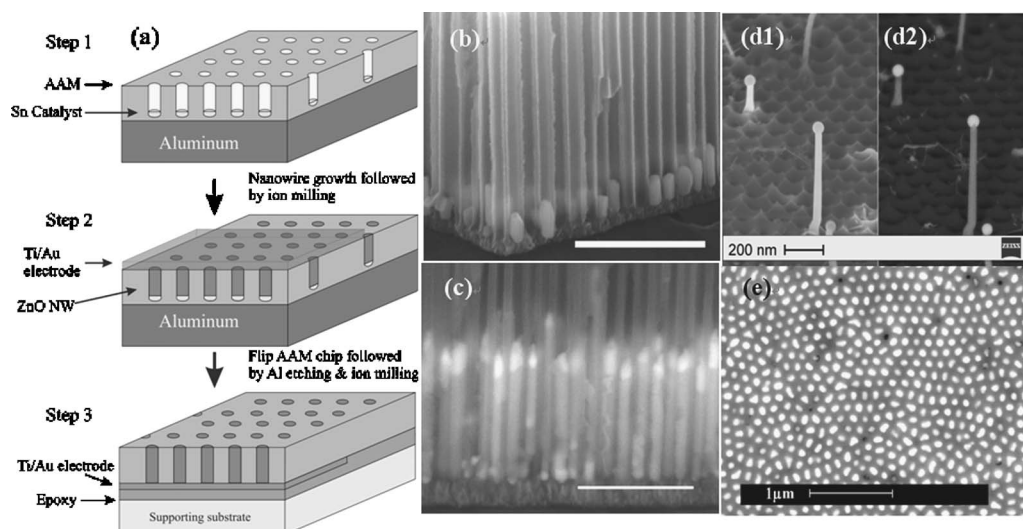


FIG. 2. (a) Schematic of the process for fabricating a vertical ZnO nanowire array with a bottom contact electrode. (b) Cross section of an AAM shows the Sn deposited at the bottom of the pores. Scale bar: $1\ \mu\text{m}$. (c) Cross section of an AAM reveals ZnO nanowires grown for 5 min by CVD. Scale bar: $1\ \mu\text{m}$. (d1) SEM and (d2) BSE (Zeiss, Ultra 55) images of vertical ZnO nanowires capped with Sn nanoparticles. (e) Top view of a ZnO nanowire array embedded in an AAM after ion milling.

electrode fabrication procedure is illustrated in Fig. 2(a). In the first step, Sn catalyst was deposited into the bottom of the AAM channels via alternating current electrodeposition at 50 Hz and 4.5 V in a mixture of 70 g/l $\text{SnCl}_2 \cdot 2\text{H}_2\text{O}$ and 400 g/l sodium citrate. Cross-section FESEM image [Fig. 2(b)] demonstrates that short Sn nanowires were deposited at the bottom of the AAM channels with length around 300 nm. In the second step, the AAM/aluminum chip was placed into a horizontal furnace using a similar CVD setup as reported before¹⁰ to perform the nanowire growth at 500 °C and 0.8 Torr. In addition, a pulsed Nd:YAG (yttrium aluminum garnet) laser was used at 0.1 Hz repetition rate to ablate Zn powder from upstream to increase Zn vapor concentration. Figure 2(c) demonstrates a backscattered electron (BSE) image taken from the cross section of an AAM after 10 min CVD growth in which the brightness reflects the atomic mass difference. It clearly shows that the nanowires grown in AAM are capped with a heavier atomic mass nanoparticle. After half an hour of CVD growth, it was found that large numbers of vertical nanowires were grown out of the AAM pores, as shown in Fig. 2(d). High resolution transmission electron microscopy and energy dispersive x-ray microanalysis studies have further revealed that these nanowires are single crystalline ZnO nanowires grown along the [001] direction and the nanoparticles are composed of Sn metal. These observations are in agreement with the results reported by Gao *et al.*¹¹ indicating that the nanowire growth was governed by a vapor-liquid-solid mechanism.

After the CVD process, the AAM/aluminum chip was subject to ion milling for 30 min to remove the nanowires on the AAM surface. The FESEM image shown in Fig. 2(e) reveals that most of the pores are filled with nanowires. Thereafter, 20 nm Ti and 180 nm Au films were patterned onto the AAM using a shadow mask followed by electron beam evaporation, as illustrated in step 2 of Fig. 2(a). In order to study the electrical property of the individual nanowires embedded in AAM, the entire AAM/aluminum chip was flipped and bonded to a supporting glass substrate using epoxy, as shown in step 3 of Fig. 2(a). The aluminum was

then removed using a saturated HgCl_2 solution and the sub-channel layer was removed by ion milling.

In this work, the interpore distance of the AAM channels is 150 nm determined by the anodization voltage used. In principle, an interpore distance of 25 nm can be readily achieved, yielding a channel density of $\sim 10^{12}$ per square inch. Such high density nanowire arrays have promising potential for constructing nanoscale integrated circuits. As a foundation to investigate the electrical properties of the individual ZnO nanowires in AAM, a conductive AFM probe was placed on top of an individual nanowire, maintaining electrical contact with a contact force of $2.4\ \mu\text{N}$. The bottom electrode was grounded, as depicted in Fig. 3(a). To investigate the role of the probe metal coating on the electrical transport across this metal/semiconductor (M/SC) point con-

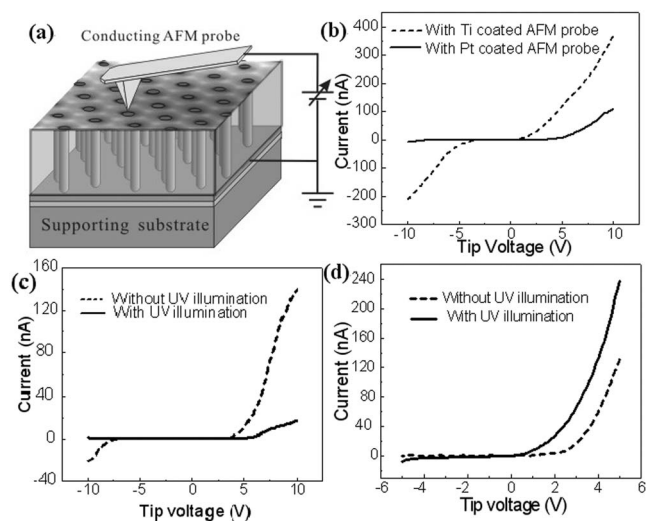


FIG. 3. (a) Schematic of using an AFM probe to address and measure individual ZnO nanowires in a vertical nanowire array. The top layer is an actual SEM image of an AAM. (b) I - V curves obtained from a vertical nanowire using conductive AFM probes with Ti and Pt coating, respectively. (c) I - V curves obtained from a vertical nanowire grown in an unannealed AAM. (d) I - V curves obtained using conductive AFM with and without UV illumination from a single nanowire grown in an annealed AAM.

tact, conductive probes with both Pt and Ti coatings were utilized. Figure 3(b) exhibits the current-voltage (I - V) curves obtained on an individual nanowire which are Schottky in nature and the one obtained using a Pt coated probe exhibits a larger barrier compared to the one acquired with a Ti coated probe. This is a result of the different work functions (ϕ) of Ti (4.31 eV) and Pt (5.56 eV), leading to a lower contact potential barrier between Ti and the n -type ZnO ($\phi = 4.2$ eV). The asymmetry in the I - V curves is attributed to increased band bending at the surface of the n -type ZnO nanowire when applied with a negative tip voltage.¹² Compared with the electrical measurement performed on free-standing ZnO nanorods,¹³ the level of the electrical current obtained in our experiment is much higher on AAM-embedded nanowires. This accrues mainly from the better M/SC contact due to the higher contact force, as well as the selection of the metal electrode. In addition, the unique structure in which the semiconducting nanowires are embedded inside the Al₂O₃ membrane prevents surface adsorption of chemicals that can significantly reduce the conductance.¹⁴

ZnO nanowires are known as promising candidates for nanoscale light detection.^{15,16} The UV detection characteristic of individual vertical ZnO nanowires was investigated to explore their potential for integrated nanoscale optoelectronics. Specifically, a nanowire array was illuminated with a UV lamp (300–425 nm, ~ 6 mW/cm²), while the electric current was recorded by a conductive AFM probe with Pt coating in contact with a nanowire. Figure 3(c) plots the I - V curves obtained with and without UV illumination. These curves illustrate a pronounced optical switching effect with one order of magnitude conductance change at 10 V bias voltage. Interestingly, in contrast to the previous report,¹⁵ UV illumination significantly reduces the conductance of the nanowire. This negative photoconductive behavior is ascribed to electron trapping in AAM. It is known that AAM is composed of an acid-anion-containing alumina layer and a pure alumina layer^{17,18} corresponding to the inner and outer oxide layers, respectively. It was reported that the anion impurities introduce electron trapping states in the inner oxide layer.¹⁹ Since the ZnO nanowires are tightly surrounded by the inner oxide layer forming a core-shell heterostructure, their electron wave functions overlap into the states in the inner oxide layer. The observation of the negative photoconductivity indicates that some of these trapping states have energy levels higher than the conduction band in the nanowires. Electrons can thus tunnel into these trapping states under photon excitation leading to the reduction of the conduction electron concentration in the nanowire channel. In addition, the trapped electrons in the inner oxide layer produce a negative surrounding gating effect, thus further decreasing the nanowire conductance. The anomalous optoelectronic switching effect from the vertical ZnO nanowires is essentially the outcome of the interaction between the nanowire and the surrounding impure alumina. Therefore, one can reason that a positive switching effect should be observed if the surface of the inner oxide layer is conformally coated with a layer of high purity Al₂O₃ or using thermal annealing to decompose the acid anion thus reduce the impurity levels in the inner oxide layer.²⁰ In order to verify this rationale, an AAM was thermally annealed at 500 °C for

13 h in 1 atm pure Ar environment. Then the ZnO nanowire array was grown inside the membrane, and the bottom contact electrode was fabricated following the procedures described above. The I - V curves obtained with and without UV illumination on a single nanowire using AFM are shown in Fig. 3(d), which clearly demonstrate the positive photoconductivity.

In conclusion, high density vertical ZnO nanowire arrays are fabricated via electrodeposition in conjunction with chemical vapor deposition method. The electrical and photoconductive properties of individual nanowires were characterized with conductive AFM probe. Combining with high resolution lithographic techniques to address individual nanowires, the nanowire arrays can be fabricated into even more complex circuits and devices such as logic gates, photonic crystals, ultrahigh resolution imaging sensors, and display devices.

The authors would like to thank Dawei Wang for technical assistance and Guorong Chen for valuable discussions. This work was supported by NSF Grant Nos. ECS-0306735 and EEC-0210120 and by the Research Institute of Matter Regularity.

¹M. Law, L. E. Greene, J. C. Johnson, R. Saykally, and P. D. Yang, *Nat. Mater.* **4**, 455 (2005).

²H. T. Ng, J. Han, T. Yamada, P. Nguyen, Y. P. Chen, and M. Meyyappan, *Nano Lett.* **4**, 1247 (2004).

³L. Gangloff, E. Minoux, K. B. K. Teo, P. Vincent, V. T. Semet, V. T. Binh, M. H. Yang, I. Y. Y. Bu, R. G. Lacerda, G. Pirio, J. P. Schnell, D. Pribat, D. G. Hasko, G. A. J. Amaratunga, W. I. Milne, and P. Legagneux, *Nano Lett.* **4**, 1575 (2004).

⁴T. Martensson, M. Borgstrom, W. Seifert, B. J. Ohlsson, and L. Samuelson, *Nanotechnology* **14**, 1255 (2003).

⁵T. Martensson, P. Carlberg, M. Borgstrom, L. Montelius, W. Seifert, and L. Samuelson, *Nano Lett.* **4**, 699 (2004).

⁶A. Johansson, E. Widenkvist, J. Lu, M. Boman, and U. Jansson, *Nano Lett.* **5**, 1603 (2005).

⁷J. S. Jie, G. Z. Wang, Q. T. Wang, Y. M. Chen, X. H. Han, X. P. Wang, and J. G. Hou, *J. Phys. Chem. B* **108**, 11976 (2004).

⁸T. Yanagishita, M. Sasaki, K. Nishio, and H. Masuda, *Adv. Mater. (Weinheim, Ger.)* **16**, 429 (2004).

⁹K. Nielsch, F. Muller, A. P. Li, and U. Gosele, *Adv. Mater. (Weinheim, Ger.)* **12**, 582 (2000).

¹⁰P. C. Chang, Z. Y. Fan, D. W. Wang, W. Y. Tseng, W. A. Chiou, J. Hong, and J. G. Lu, *Chem. Mater.* **16**, 5133 (2004).

¹¹P. X. Gao, Y. Ding, and Z. L. Wang, *Nano Lett.* **3**, 1315 (2003).

¹²*Scanning Tunneling Microscopy and Spectroscopy: Theory, Techniques, and Applications*, 2nd ed., edited by Dawn A. Bonnelli (Wiley-VCH, New York, 2001).

¹³W. I. Park, G. C. Yi, J. W. Kim, and S. M. Park, *Appl. Phys. Lett.* **82**, 4358 (2003).

¹⁴Z. Y. Fan, D. W. Wang, P. C. Chang, W. Y. Tseng, and J. G. Lu, *Appl. Phys. Lett.* **85**, 5923 (2004).

¹⁵H. Kind, H. Q. Yan, B. Messer, M. Law, and P. D. Yang, *Adv. Mater. (Weinheim, Ger.)* **14**, 158 (2002).

¹⁶Z. Y. Fan, P. C. Chang, J. G. Lu, E. C. Walter, R. M. Penner, C. H. Lin, and H. P. Lee, *Appl. Phys. Lett.* **85**, 6128 (2004).

¹⁷J. Choi, Y. Luo, R. B. Wehrspohn, R. Hillebrand, J. Schilling, and U. Gosele, *J. Appl. Phys.* **94**, 4757 (2003).

¹⁸Y. Yamamoto, N. Baba, and S. Tajima, *Nature (London)* **289**, 572 (1981).

¹⁹N. Kouklin, L. Menon, A. Z. Wong, D. W. Thompson, J. A. Woollam, P. F. Williams, and S. Bandyopadhyay, *Appl. Phys. Lett.* **79**, 4423 (2001).

²⁰G. Xiong, J. W. Elam, H. Feng, C. Y. Han, H. H. Wang, L. E. Iton, L. A. Curtiss, M. J. Pellin, M. Kung, H. Kung, and P. C. Stair, *J. Phys. Chem. B* **109**, 14059 (2005).